

Decentralized Federated Learning through Proxy Model Sharing

Shivam Kalra^{1,2,3*} Junfeng Wen^{4*†} Jesse C. Cresswell^{1*}
Maksims Volkovs¹ Hamid R. Tizhoosh^{2,3,5}

¹Layer 6 AI

²Kimia Lab, University of Waterloo

³Vector Institute

⁴Carleton University

⁵Rhazes Lab, Mayo Clinic

shivam.kalra@uwaterloo.ca, {junfeng, jesse, maks}@layer6.ai, tizhoosh.hamid@mayo.edu

Abstract

Institutions in highly regulated domains such as finance and healthcare often have restrictive rules around data sharing. Federated learning is a distributed learning framework that enables multi-institutional collaborations on decentralized data with improved protection for each collaborator’s data privacy. In this paper, we propose a communication-efficient scheme for decentralized federated learning called ProxyFL, or proxy-based federated learning. Each participant in ProxyFL maintains two models, a private model, and a publicly shared proxy model designed to protect the participant’s privacy. Proxy models allow efficient information exchange among participants without the need of a centralized server. The proposed method eliminates a significant limitation of canonical federated learning by allowing model heterogeneity; each participant can have a private model with any architecture. Furthermore, our protocol for communication by proxy leads to stronger privacy guarantees using differential privacy analysis. Experiments on popular image datasets, and a cancer diagnostic problem using high-quality gigapixel histology whole slide images, show that ProxyFL can outperform existing alternatives with much less communication overhead and stronger privacy.

1 Introduction

Access to large-scale datasets is a primary driver of advancement in machine learning, with well-known datasets such as ImageNet [Deng et al., 2009] in computer vision, or SQuAD [Rajpurkar et al., 2016] in natural language processing leading to remarkable achievements. Other domains such as healthcare and finance face restrictions on sharing data, due to regulations and privacy concerns. It is impossible for institutions in these domains to pool and disseminate their data, which limits the progress of research and model development. The ability to share information between institutions while respecting the data privacy of individuals would lead to more robust and accurate models.

In the healthcare domain, for example, histopathology has seen widespread adoption of digitization, offering unique opportunities to increase objectivity and accuracy of diagnostic interpretations through machine learning [Tizhoosh and Pantanowitz, 2018]. Digital images of tissue specimens exhibit significant heterogeneity from the preparation, fixation and staining protocols used at the preparation site, among other factors. Without careful regularization, deep models may excessively focus on imaging artifacts and hence fail to generalize on data collected from new sources [Cohen et al., 2021]. Additionally, the need to serve a diverse population including minority or rare groups [McCoy et al., 2020], and mitigate

*Equal contribution.

†Work done while at Layer 6 AI.

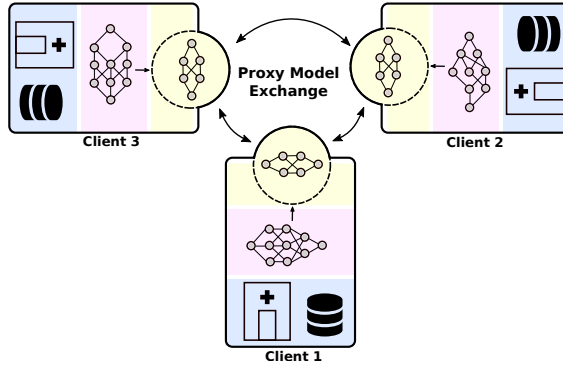


Figure 1: *ProxyFL* is a communication-efficient, decentralized federated learning method where each client (e.g. hospital) maintains a private model, a proxy model, and private data. During distributed training, the client communicates with others only by exchanging their proxy model which enables data and model autonomy. After training, a client’s private model can be used for inference.

bias Vokinger et al. [2021], requires diverse and multi-centric datasets for model training. Because of specializations at institutions and variability across local populations the integration of medical data across multiple institutions is essential.

However, centralization of medical data faces regulatory obstacles, as well as workflow and technical challenges including managing and distributing the data. The latter is particularly relevant for digital pathology since each histopathology image is generally a gigapixel file, often one or more gigabytes in size. Distributed machine learning on decentralized data could be a solution to overcome these challenges, and promote the adoption of machine learning in healthcare and similar highly regulated domains.

Federated learning (FL) is a distributed learning framework that was designed to train a model on data that could not be centralized [McMahan et al., 2017]. It trains a model in a distributed manner directly on client devices where data is generated, and gradient updates are communicated back to the centralized server for aggregation. However, the centralized FL setting is not suited to the multi-institutional collaboration problem, as it involves a centralized third party that controls a single model. Considering a collaboration between hospitals, creating one central model may be undesirable. Each hospital may seek autonomy over its own model for regulatory compliance and tailoring to its own specialty. As a result, decentralized FL frameworks [Li et al., 2020a] are preferred under such settings.

While it is often claimed that FL provides improved privacy since raw data never leaves the client’s device [McMahan et al., 2017], it does not provide the guarantee of security that regulated institutions require. FL involves each client sending unaudited gradient updates to the central server, which is problematic since deep neural networks are capable of memorizing individual training examples, which may completely breach the client’s privacy [Carlini et al., 2019].

In contrast, meaningful and quantitative guarantees of privacy are provided by the differential privacy (DP) framework [Dwork et al., 2006b]. In DP, access to a database is only permitted through randomized queries in a way that obscures the presence of individual data points. More formally, let \mathcal{D} represent a set of data points, and M a probabilistic function, or *mechanism*, acting on databases. We say that the mechanism is (ϵ, δ) -*differentially private* if for all subsets of possible outputs $\mathcal{S} \subset \text{Range}(M)$, and for all pairs of databases \mathcal{D} and \mathcal{D}' that differ by one element,

$$\Pr[M(\mathcal{D}) \in \mathcal{S}] \leq \exp(\epsilon) \Pr[M(\mathcal{D}') \in \mathcal{S}] + \delta. \quad (1)$$

The spirit of this definition is that when one individual’s data is added or removed from the database, the outcomes of a private mechanism should be largely unchanged in distribution. This will hold when ϵ and δ are small positive numbers. In this case an adversary would not be able to learn about the individual’s data by observing the mechanism’s output, hence, privacy is preserved. DP mechanisms satisfy several useful properties, including strong guarantees of privacy under composition, and post-processing [Dwork and Roth, 2014, Dwork et al., 2010]. However, if an individual contributes several datapoints to a dataset, then their privacy guarantees may be weaker than expected due to correlations between their datapoints. Still, *group differential privacy* [Dwork and Roth, 2014] shows that privacy guarantees degrade in a controlled

manner as the number of datapoints contributed increases. These properties make DP a suitable solution for ensuring data privacy in a collaborative FL setting.

In this work, we propose proxy-based federated learning, or ProxyFL, for decentralized collaboration between institutions which enables training of high-performance and robust models, without sacrificing data privacy or communication efficiency. Our contributions are: (i) a method for decentralized FL in multi-institutional collaborations that is adapted to heterogeneous data sources, and preserves model autonomy for each participant; (ii) incorporation of DP for rigorous privacy guarantees; (iii) analysis and improvement of the communication overhead required to collaborate.

2 Related Work

Decentralized FL for highly regulated domains. Unlike centralized FL [McMahan et al., 2017, Li et al., 2020a] where federated clients coordinate to train a centralized model that can be utilized by everyone as a service, decentralized FL is more suitable for multi-institutional collaborations due to regulatory constraints. The main challenge of decentralized FL is to develop a protocol that allows information passing in a peer-to-peer manner. Gossip protocols [Kempe et al., 2003] can be used for efficient communication and information sharing [Nedić and Olshevsky, 2016, Nedić et al., 2018]. There are different forms of information being exchanged in the literature, including model weights [Li et al., 2022, Huang et al., 2021], knowledge representations [Wittkopp and Acker, 2020] or model outputs [Lin et al., 2020, Ma et al., 2021]. However, unlike our method, none of these protocols provides a quantitative theoretical guarantee of privacy for participants, and therefore are not suitable for highly regulated domains.

Several other methods have been proposed to achieve decentralization with varying secondary objectives. In Cyclical Weight Transfer (CWT) [Chang et al., 2018] each client trains a model on local data, then passes that model to the next client in a cyclical fashion. Like standard FL, CWT avoids the need to centralize data and can achieve good performance when strict privacy (à la DP) is not a concern. Split learning [Gupta and Raskar, 2018] enables multiple parties to jointly train a single model with a server such that no party controls the entire model. In our context, the additional reliance on a central party for inference is undesirable. Finally, swarm learning [Warnat-Herresthal et al., 2021] applies blockchain technology to promote a decentralized, secure network for collaborative training, with one client voted in to act as a central authority each round. Swarm learning does not change the core learning algorithm of FL [McMahan et al., 2017] so it inherits relatively poor model performance when strict privacy measures are applied, and requires homogeneous model architectures.

Mutual learning. Each client in our ProxyFL has two models that serve different purposes. They are trained using a DP variant of deep mutual learning (DML) [Zhang et al., 2018] which is an approach for mutual knowledge transfer. DML compares favourably to knowledge distillation between a pre-trained teacher and a typically smaller student [Hinton et al., 2015] since it allows training both models simultaneously from scratch, and provides beneficial information to both models. Federated Mutual Learning (FML) [Shen et al., 2020] introduces a meme model that resembles our proxy model, which is also trained mutually with each client’s private model, but is aggregated at a central server. However, FML is not well-suited to the multi-institutional collaboration setting as it is centralized and provides no privacy guarantee to clients.

Differential privacy in FL. Although raw data never leaves client devices, FL is still susceptible to breaches of privacy [Melis et al., 2019, Bhowmick et al., 2018]. DP has been combined with FL to train centralized models with a guarantee of privacy for all clients that participate [McMahan et al., 2018]. By ensuring that gradient updates are not overly reliant on the information in any single training example, gradients can be aggregated centrally with a DP guarantee [Abadi et al., 2016]. We take inspiration from these ideas for ProxyFL.

Computational pathology. The main application domain considered in this work is computational pathology. Various articles have emphasized the need for privacy-preserving FL when facing large-scale computational pathology workloads. Li et al. [2019] and Ke et al. [2021] used FL for medical image augmentation and segmentation. Their method used a centralized server to aggregate selective weight updates that were treated in a DP framework, but they did not account for the total privacy budget expended over the training procedure. Li et al. [2020b] and Lu et al. [2022] built medical image classification models with FL, and added noise to model weights for privacy. However, model weights have unbounded sensitivity, so no meaningful DP guarantee is achieved with these techniques.

3 Method - ProxyFL

ProxyFL, or proxy-based federated learning is our proposed approach for decentralized federated learning. It is designed for multi-institutional collaborations in highly-regulated domains, and as such incorporates quantitative privacy guarantees with efficient communication.

3.1 Problem Formulation & Overview

We consider the decentralized FL setting involving a set of clients \mathcal{K} , each with a local data distribution $\mathcal{D}_k, \forall k \in \mathcal{K}$. Every client maintains a private model $f_{\phi_k} : \mathcal{X} \rightarrow \mathcal{Y}$ with parameters ϕ_k , where \mathcal{X}, \mathcal{Y} are the input/output spaces respectively. In this work, we assume that all private models have the same input/output specifications, but may have different structures (this can be further relaxed by including client-specific input/output adaptation layers). The goal is to train the private models collectively so that each generalizes well on the joint data distribution.

There are three major challenges in this setting: (i) The clients may not want to reveal their private model’s structure and parameters to others. Revealing model structure can expose proprietary information, increase the risk of adversarial attacks [Fredrikson et al., 2015], and can leak private information about the local datasets [Truex et al., 2019]. (ii) In addition to model heterogeneity, the clients may not want to rely on a third party to manage a shared model, which precludes centralized model averaging schemes. (iii) Information sharing must be efficient, robust, and peer-to-peer. To address the above challenges, we introduce an additional proxy model $h_{\theta_k} : \mathcal{X} \rightarrow \mathcal{Y}$ for each client with parameters θ_k . It serves as an interface between the client and the outside world. As part of the communication protocol, all clients agree on a common proxy model architecture for compatibility. Proxy models enable architectural independence among federated clients that may enhance security against white-box adversarial attacks in which the attacker has knowledge of the model architecture [Carlini and Wagner, 2017]. The proxy model is generally smaller than the private model thus reducing communication overhead among clients. Furthermore, diverting all shared information through the proxy allows the private model to be trained without DP. Since DP incurs a loss of utility, the private model, which is ultimately used for inference by the client locally, tends to have much higher accuracy than otherwise.

In every round of ProxyFL, each client trains its private and proxy models jointly so that they can benefit from one another. With differentially private training, the proxy can extract useful information from private data, ready to be shared with other clients without violating privacy constraints. Then, each client sends its proxy to its out-neighbors and receives new proxies from its in-neighbors according to a communication graph, specified by an adjacency matrix P and de-biasing weights w . Finally, each client aggregates the proxies they received, and replaces their current proxy. The overall procedure is shown in Fig. 1 and Algorithm 1. We discuss each step in detail in the subsequent subsections.

3.2 Training Objectives

For concreteness, we consider classification tasks. To train the private and proxy models at the start of each round of training, we apply a variant of DML [Zhang et al., 2018]. Specifically, when training the private model for client k , in addition to the cross-entropy loss (CE)

$$\mathcal{L}_{\text{CE}}(f_{\phi_k}) := \mathbb{E}_{(\mathbf{x}, y) \sim \mathcal{D}_k} \text{CE}[f_{\phi_k}(\mathbf{x}) \| y], \quad (2)$$

DML adds a KL divergence loss (KL)

$$\mathcal{L}_{\text{KL}}(f_{\phi_k}; h_{\theta_k}) := \mathbb{E}_{(\mathbf{x}, y) \sim \mathcal{D}_k} \text{KL}[f_{\phi_k}(\mathbf{x}) \| h_{\theta_k}(\mathbf{x})], \quad (3)$$

so that the private model can also learn from the current proxy model. The objective for learning the private model is given by

$$\mathcal{L}_{\phi_k} := (1 - \alpha) \cdot \mathcal{L}_{\text{CE}}(f_{\phi_k}) + \alpha \cdot \mathcal{L}_{\text{KL}}(f_{\phi_k}; h_{\theta_k}), \quad (4)$$

where $\alpha \in (0, 1)$ balances between the two losses. The objective for the proxy model is similarly defined as

$$\mathcal{L}_{\theta_k} := (1 - \beta) \cdot \mathcal{L}_{\text{CE}}(h_{\theta_k}) + \beta \cdot \mathcal{L}_{\text{KL}}(h_{\theta_k}; f_{\phi_k}). \quad (5)$$

Algorithm 1: ProxyFL

Require: Proxy parameters $\theta_k^{(0)}$, private parameters $\phi_k^{(0)}$, de-biasing weight $w_k^{(0)}$ for client k , DML weights $\alpha, \beta \in (0, 1)$, learning rate $\eta > 0$, adjacency matrix $P^{(t)}$

- 1 **for** each round $t = 0, \dots, T - 1$ at client $k \in \mathcal{K}$ **do**
- 2 **for** each local optimization step **do**
- 3 Sample mini-batch $\mathcal{B}_k = \{(\mathbf{x}_i, y_i)\}_{i=1}^B$ from \mathcal{D}_k ;
- 4 Update local proxy and private models:

$$\theta_k^{(t)} \leftarrow \theta_k^{(t)} - \eta \tilde{\nabla} \widehat{\mathcal{L}}_{\theta_k}(\mathcal{B}_k) \quad \# \text{ DP update}$$

$$\phi_k^{(t)} \leftarrow \phi_k^{(t)} - \eta \nabla \widehat{\mathcal{L}}_{\phi_k}(\mathcal{B}_k) \quad \# \text{ non-DP update}$$
- 5 **end**
- 6 $\phi_k^{(t+1)} \leftarrow \phi_k^{(t)}$;
- 7 Send $(P_{k',k}^{(t)} \theta_k^{(t)}, P_{k',k}^{(t)} w_k^{(t)})$ to out-neighbors;
- 8 receive $(P_{k,k'}^{(t)} \theta_{k'}^{(t)}, P_{k,k'}^{(t)} w_{k'}^{(t)})$ from in-neighbors;
- 9 Update local proxy $\theta_k^{(t+1)} \leftarrow \sum_{k'} P_{k,k'}^{(t)} \theta_{k'}^{(t)}$;
- 10 Update de-biasing weight $w_k^{(t+1)} \leftarrow \sum_{k'} P_{k,k'}^{(t)} w_{k'}^{(t)}$;
- 11 De-bias $\theta_k^{(t+1)} \leftarrow \theta_k^{(t+1)} / w_k^{(t+1)}$;
- 12 **end**
- 13 **return** $\theta_k^{(T)}, \phi_k^{(T)}$;

where $\beta \in (0, 1)$. As in DML, we alternate stochastic gradient steps between the private and proxy models.

In our context, mini-batches are sampled from the client's private dataset. Releasing the proxy model to other clients risks revealing that private information. Therefore, each client uses differentially private stochastic gradient descent (DP-SGD) [Abadi et al., 2016] when training the proxy (but not the private model). Let $\mathcal{B}_k = \{(\mathbf{x}_i, y_i)\}_{i=1}^B$ denote a mini-batch sampled from \mathcal{D}_k . The stochastic gradient is $\nabla \widehat{\mathcal{L}}_{\phi_k}(\mathcal{B}_k) := \frac{1}{B} \sum_{i=1}^B \mathbf{g}_{\phi_k}^{(i)}$ where

$$\mathbf{g}_{\phi_k}^{(i)} := (1 - \alpha) \nabla_{\phi_k} \text{CE}[f_{\phi_k}(\mathbf{x}_i) \| y_i] + \alpha \nabla_{\phi_k} \text{KL}[f_{\phi_k}(\mathbf{x}_i) \| h_{\theta_k}(\mathbf{x}_i)]. \quad (6)$$

$\nabla \widehat{\mathcal{L}}_{\theta_k}(\mathcal{B}_k)$ and $\mathbf{g}_{\theta_k}^{(i)}$ are similarly defined for the proxy. To perform DP training for the proxy, the per-example gradient is clipped, then aggregated over the mini-batch, and finally Gaussian noise is added [Abadi et al., 2016]:

$$\begin{aligned} \bar{\mathbf{g}}_{\theta_k}^{(i)} &:= \mathbf{g}_{\theta_k}^{(i)} / \max\left(1, \|\mathbf{g}_{\theta_k}^{(i)}\|_2 / C\right), \\ \tilde{\nabla} \widehat{\mathcal{L}}_{\theta_k}(\mathcal{B}_k) &:= \frac{1}{B} \left(\sum_{i=1}^B \bar{\mathbf{g}}_{\theta_k}^{(i)} + \mathcal{N}(0, \sigma^2 C^2 I) \right), \end{aligned} \quad (7)$$

where $C > 0$ is the clipping threshold and $\sigma > 0$ is the noise level (see Lines 2–5 in Algorithm 1).

3.3 Privacy Guarantee

The proxy model is the only entity that a client reveals, so each client must ensure this sharing does not compromise the privacy of their data. Since arbitrary post-processing on a DP-mechanism does not weaken its (ϵ, δ) guarantee [Dwork and Roth, 2014], it is safe to release the proxy as long as it was trained via a DP-mechanism. DP-SGD as defined in Eq. (7) is based on the Gaussian mechanism [Dwork et al., 2006a] which meets the requirement of Eq. (1) by adding Gaussian noise to the outputs of a function f with bounded sensitivity C in L_2 norm,

$$M(x) = f(x) + \mathcal{N}(0, \sigma^2 C^2 I). \quad (8)$$

DP-SGD simply takes $f(x)$ to be the stochastic gradient update, with clipping to ensure bounded sensitivity.

Every application of the DP-SGD step incurs a privacy cost related to the clipping threshold C , and noise level σ . A strong bound on the total privacy cost over many applications of DP-SGD is obtained by using the framework of Rényi differential privacy [Mironov, 2017, Mironov et al., 2019] to track privacy under compositions of DP-SGD, then convert the result to the language of (ϵ, δ) -DP as in Eq. (1) [Balle et al., 2020].

Finally, privacy guarantees are tracked on a per-client basis. In a multi-institutional collaboration, every client has an obligation to protect the privacy of the data it has collected. Hence, each client individually tracks the parameters (ϵ, δ) for its own proxy model training, and can drop out of the protocol when its prespecified privacy budget is reached. Throughout the paper we specify δ based on the dataset size, and compute ϵ .

3.4 Communication Efficiency & Robustness

The proxies serve as interfaces for information transfer and must be locally aggregated in a way that facilitates efficient learning among clients. One may use a central parameter server to compute the average of the proxies, similar to Shen et al. [2020]. However, this will incur a communication cost that grows linearly in the number of clients, and is not decentralized. We propose to apply the PushSum scheme [Kempe et al., 2003, Nedić et al., 2018] to exchange proxies among clients that significantly reduces the communication overhead.

Let $\Theta^{(t)} \in \mathbb{R}^{|\mathcal{K}| \times d_\theta}$ represent the stacked proxies at round t , where the rows are the proxy parameters $\theta_k^{(t)}, \forall k \in \mathcal{K}$. We use $P^{(t)} \in \mathbb{R}^{|\mathcal{K}| \times |\mathcal{K}|}$ to denote the weighted adjacency matrix representing the graph topology at round t , where $P_{k,k'}^{(t)} \neq 0$ indicates that client k receives the proxy from client k' . Note that $P^{(t)}$ needs to be column-stochastic, but need not be symmetric (bidirectional communication) nor time-invariant (across rounds). Such a $P^{(t)}$ will ensure efficient communication when it is sparse. The communication can also handle asymmetrical connections such as different upload/download speeds, and can adapt to clients joining or dropping out since it is time-varying.

With these notations, every round of communication can be concisely written as $\Theta^{(t+1)} = P^{(t)}\Theta^{(t)}$. Under certain mixing conditions [Seneta, 2006], it can be shown that $\lim_{T \rightarrow \infty} \prod_{t=0}^T P^{(t)} = \pi \mathbf{1}^\top$, where π is the limiting distribution of the Markov chain and $\mathbf{1}$ is a vector of all ones. Suppose for now that there is no training for the proxies between rounds, i.e., updates to the proxies are due to communication and replacement only. In the limit, θ_k will converge to $\theta_k^{(\infty)} = \pi_k \sum_{k' \in \mathcal{K}} \theta_{k'}^{(0)}$. To mimic model averaging (i.e., computing $\frac{1}{|\mathcal{K}|} \sum_{k' \in \mathcal{K}} \theta_{k'}^{(0)}$), the bias introduced by π_k must be corrected. This can be achieved by having the clients maintain another set of weights $\mathbf{w} \in \mathbb{R}^{|\mathcal{K}|}$ with initial values $\mathbf{w}^{(0)} = \mathbf{1}$. By communicating $\mathbf{w}^{(t+1)} = P^{(t)}\mathbf{w}^{(t)}$, we can see that $\mathbf{w}^{(\infty)} = \pi \mathbf{1}^\top \mathbf{w}^{(0)} = |\mathcal{K}| \pi$. As a result, the de-biased average is given by $\theta_k^{(\infty)} / w_k^{(\infty)} = \frac{1}{|\mathcal{K}|} \sum_{k' \in \mathcal{K}} \theta_{k'}^{(0)}$.

Finally, recall that the proxies are trained locally in each round. Instead of running the communication to convergence for proxy averaging, we alternate between training (Lines 2–5 in Algorithm 1) and communicating (Lines 7–10) proxies, similar to Assran et al. [2019].

4 Empirical Evaluation

In this section, we demonstrate the effectiveness and efficiency of ProxyFL on popular image classification datasets as well as a cancer diagnostic problem. In our experiments, we use the exponential communication protocol of Assran et al. [2019], as illustrated in Fig. 2. The communication graph $P^{(t)}$ is a permutation matrix so that each client only receives and sends one proxy per communication round. Each client communicates with its peer that is $2^0, 2^1, \dots, 2^{\lfloor \log_2(|\mathcal{K}|-1) \rfloor}$ steps away periodically. Sending only one proxy per communication round enables ProxyFL to scale to large numbers of clients. The communication and synchronization is handled via the OpenMPI library [Graham et al., 2005]. Our code is available at <https://github.com/layer6ai-labs/ProxyFL>.

4.1 Benchmark Image Classification

Datasets & settings. We conducted experiments on MNIST [LeCun et al., 1998], Fashion-MNIST (FaMNIST) [Xiao et al., 2017] and CIFAR-10 [Krizhevsky, 2009]. MNIST and FaMNIST have 60k training

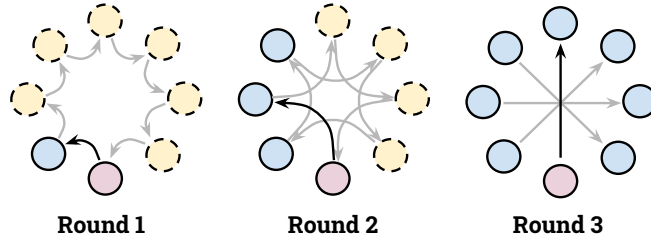


Figure 2: An illustration of the directed exponential graphs used in our experiments. Dark arrows indicate the communication path of the bottom node at each round, while light arrows show the communication path of others. Solid nodes indicate clients who have received information from the bottom client. After only $\lceil \log_2(|\mathcal{K}|) \rceil$ rounds, all nodes have access to that information.

images of size 28×28 , while CIFAR-10 has 50k RGB training images of size 32×32 . Each dataset has 10k test images, which are used to evaluate the model performance. Experiments were conducted on a server with 8 V100 GPUs, which correspond to 8 clients. In each run, every client had 1k (MNIST and FaMNIST) or 3k (CIFAR-10) non-overlapping private images sampled from the training set, meaning only a subset of the available training data was used overall which increases the difficulty of the classification task. To test robustness on non-IID data, clients were given a skewed private data distribution. For each client, a randomly chosen class was assigned and a fraction p_{major} (0.8 for MNIST and FaMNIST; 0.3 for CIFAR-10) of that client’s private data was drawn from that class. The remaining data was randomly drawn from all other classes in an IID manner. Hence, clients must learn from collaborators to generalize well on the IID test set.

Baselines. We compare our method to FedAvg [McMahan et al., 2017], FML [Shen et al., 2020], AvgPush, CWT [Chang et al., 2018], Regular, and Joint training. FedAvg and FML are centralized schemes that average models with identical structure. FML is similar to ProxyFL in that every client has two models, except FML does centralized averaging and originally did not incorporate DP training. AvgPush is a decentralized version of FedAvg using PushSum for aggregation. CWT is similar to AvgPush, but uses cyclical model passing instead of aggregation. In line with prior work [Adnan et al., 2022], we also compare federated schemes with the Regular and Joint settings. Regular training uses the local private datasets without any collaboration. Joint training mimics a scenario without constraints on data centralization by combining data from all clients and training a single model. Regular, Joint, FedAvg, AvgPush, and CWT use DP-SGD for training their models, while ProxyFL and FML use it for their proxies.

Implementation details. Following Shen et al. [2020], the private/proxy models are LeNet5/MLP for MNIST and FaMNIST, and CNN2/CNN1 for CIFAR10. All methods use the Adam optimizer [Kingma and Ba, 2014] with learning rate of 0.001, weight decay of $1e-4$, mini-batch size of 250, clipping $C = 1.0$ and noise level $\sigma = 1.0$. Each round of local training takes a number of gradient steps equivalent to one epoch over the private data. For proper DP accounting, mini-batches are sampled from the training set independently with replacement by including each training example with a fixed probability [Yu et al., 2019]. The DML parameters α, β are set at 0.5 for FML and ProxyFL. We report means and standard deviations based on 5 random seeds. Additional details and results can be found in Appendix A and B.

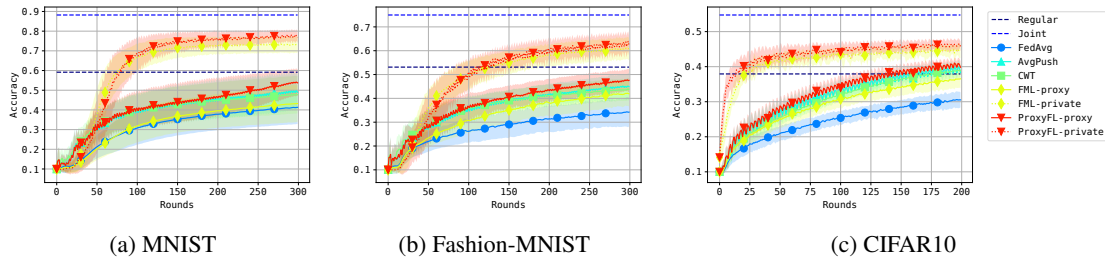


Figure 3: Test performance with differential privacy (DP) training. Datasets are, from left to right, MNIST, Fashion-MNIST, and CIFAR10. Each figure reports mean and standard deviation over 8 clients for each of 5 independent runs

Results & discussions. Fig. 3 shows the performance on the test datasets. There are a few observations: (i) The private models of ProxyFL achieve the best overall performance on all datasets, even better than the centralized counterpart FML. The improvements of ProxyFL-private over other methods are statistically significant for every dataset (p -value $< 1e-5$). Note that the Joint method serves as an upper bound of the problem when private datasets are combined. (ii) As a decentralized scheme, ProxyFL has a much lower communication cost compared to FML, as shown in Fig. 4. The exponential protocol has a constant time complexity per round regardless of the number of clients, which makes ProxyFL much more scalable. (iii) Decentralized schemes seem to be more robust to DP training, as AvgPush outperforms FedAvg and ProxyFL outperforms FML consistently.

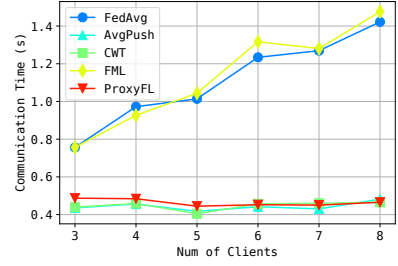


Figure 4: Communication time required as number of clients increases.

4.2 Ablation

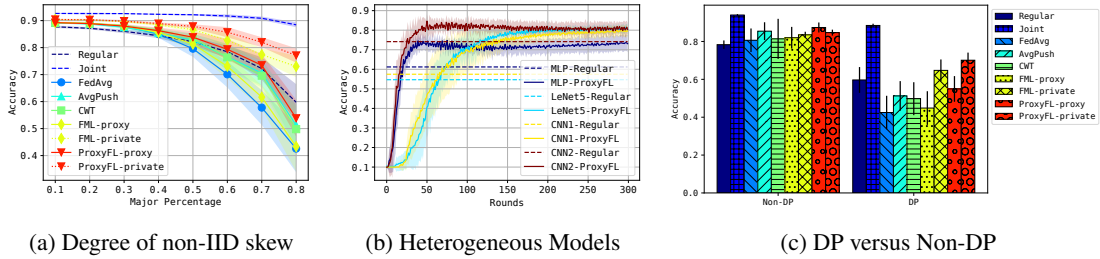


Figure 5: Ablations of our method. (a) Accuracy as the non-IID skew of the dataset increases. (b) Accuracy when clients have heterogeneous model architectures. (c) Accuracy with and without differentially private training. Each figure reports mean and standard deviation over 8 clients for each of 5 independent runs.

We ablated ProxyFL to see how different factors affect its performance on the MNIST dataset. Unless specified otherwise, all models, including the private ones in FML and ProxyFL, have the same MLP structure. Additional ablation results can be found in Appendix B.

IID versus non-IID. Fig. 5 (a) shows the performance of the methods with different levels of non-IID dataset skew. $p_{\text{major}} = 0.1$ is the IID setting because there are 10 classes. We can see that as the setting deviates from IID, most methods degrade except for Joint training since it unifies the datasets. The private model of ProxyFL is the most robust to the degree of non-IID dataset skew. Note that the proxy model of ProxyFL achieves similar performance to the private model of FML, which is trained without DP guarantees. This indicates that ProxyFL is a scheme that is robust to distribution shifts among the clients.

Different private architectures. One important aspect of ProxyFL is that the private models can be heterogeneous—customized to meet the special needs of the individual clients. On the MNIST task we use all four model architectures, one for every two clients (CNN1 and CNN2 are slightly adapted to fit MNIST images). Results are shown in Fig. 5 (b). We see that different models can achieve very diverse and sub-optimal performances with individual Regular training, while ProxyFL can improve all architectures’ performance. The improvements for weaker models are more significant than for stronger models.

DP versus non-DP. Next we investigate the effect of DP-SGD on the algorithms. Fig. 5 (c) shows the test accuracies of the different training methods with and without DP-SGD’s gradient clipping and noise addition. Clearly, all methods can outperform Regular training when there is no privacy constraint. However, with DP-SGD, centralized methods like FedAvg and FML-proxy perform poorly, even worse than Regular training. ProxyFL-private shows the smallest decrease in performance when DP-SGD is included and remains closest to the upper bound of Joint training.

4.3 Gastrointestinal Disease Detection

Dataset & setup. We applied our method on the Kvasir dataset [Pogorelov et al., 2017], which is a multi-class image dataset for gastrointestinal disease detection. It consists of 8,000 endoscopic images from eight classes such as anatomical landmarks or pathological findings. Each class has 1,000 images and each image is resized to 100×80 pixels. Following Yang et al. [2021], the dataset is partitioned into 6,000 training and 2,000 test images in each run, and the training set is further distributed into 8 clients by sampling from a Dirichlet distribution with concentration 0.5 [Yurochkin et al., 2019]. The proxy and private models are both the VGG model from Yang et al. [2021] with minor adjustments for the resized images. The parameter settings are the same as Section 4.1 except that the batch size is now 128.

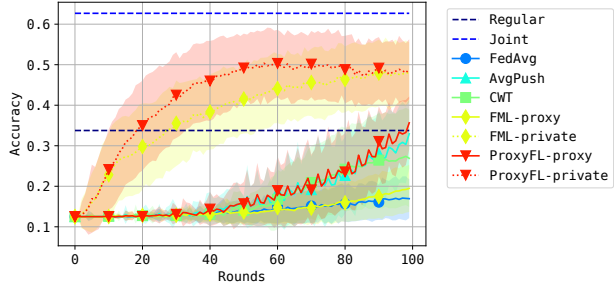


Figure 6: Test accuracy on the Kvasir dataset. This figure reports mean and standard deviation over 8 clients for each of 5 independent runs.

Results & discussion. The results are shown in Fig. 6. We can see that centralized schemes like FedAvg and FML-proxy do not learn much during the process, as opposed to their decentralized counterparts AvgPush and ProxyFL-proxy. This demonstrates the effectiveness of the PushSum scheme in this setting. Additionally, ProxyFL-private consistently outperforms FML-private during training, showing that the ProxyFL model is able to provide better learning signal to the private model compared with FML.

4.4 Histopathology Image Analysis

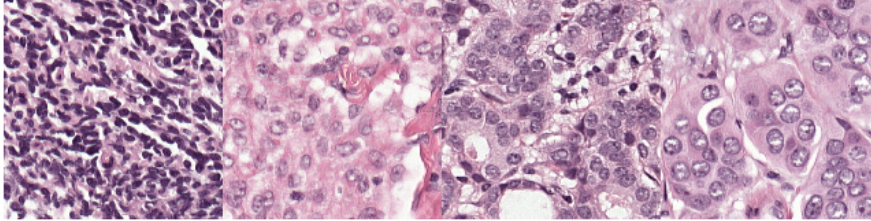


Figure 7: Patches extracted from Camelyon-17 WSIs. The first two are from healthy tissue and the latter two from WSIs containing tumors.

In this experiment, we evaluated ProxyFL for classifying the presence of lymph node metastases in a tissue sample. The presence of lymph node metastases is one of the most important factors in breast cancer prognosis. The sentinel lymph node is the most likely lymph node to contain metastasized cancer cells and is excised, histopathologically processed, and examined by the pathologist. This tedious examination process is time-consuming and can lead to small metastases being missed [Bánda et al., 2019].

Dataset. We considered a large public archive of whole-slide images (WSIs), namely the Camelyon-17 challenge dataset [Bánda et al., 2019], which has previously been used for federated learning in [Andreux et al., 2020]. The dataset is derived from 1399 annotated whole-slide images of lymph nodes, both with and without metastases. Slides were collected from five different medical centers to cover a broad range of image appearance and staining variations. A total of 209 WSIs contain detailed hand-drawn contours for all metastases. The client data for this study was created from Camelyon-17 by choosing WSIs out of these 209 annotated WSIs from four of the institutions. We used the provided annotations to extract both normal and tumor-containing patches from WSIs. We extracted 512×512 pixel patches from WSIs and assigned each patch a binary label (healthy/tumor-containing) based on the provided annotation. A similar number of patches were sampled from the WSIs originating at each of the four institutions, with balanced labels. We then split patches into training and test sets in a rough 80/20 ratio, ensuring that patches in each set originated from non-overlapping patients. The distribution of patches in each split is described in Table 1.

Generalization of models to data collected from diverse sources has become a well-known challenge for applying deep learning to medical applications [Kelly et al., 2019]. The standard method for testing

Training sets					Test set					
Label	Clients				Label	Clients				Sum
	C1	C2	C3	C4		C1	C2	C3	C4	
Healthy	1,195	1,363	1,727	1,517	Healthy	322	338	107	344	1,111
Tumor	1,143	1,363	1,210	1,324	Tumor	374	338	624	537	1,873
<i>Sum</i>	2,338	2,726	2,937	2,841	<i>Sum</i>	696	676	731	881	2,984

Table 1: Distribution of WSI patches across four different institutions. Class labels (healthy vs. tumor-containing) are defined at the WSI level, and are exactly balanced within each Client’s overall dataset. Patches in train and test sets are from non-overlapping patients, which forces some imbalance in class labels. The test sets are merged into a single multi-centric dataset for model evaluation.

generalization is to evaluate models on external test data which should originate from entirely different institutions than those used for training [Park and Han, 2018, Bizzego et al., 2019, Bluemke et al., 2020]. FL can potentially mitigate generalization problems by increasing the diversity of data that models are exposed to during training. Hence, we merged all four client test sets into a single multi-centric test set used in all model evaluations. From the perspective of a given client, a majority of the test set is external data which requires the trained model to generalize beyond the internal training data in order to show strong performance.

Models. For all methods, including both private and proxy models, we used the standard ResNet-18 neural network architecture [He et al., 2016], as implemented in the torchvision package [TorchVision, 2016], with randomly initialized weights. ResNet architectures use BatchNorm layers [Ioffe and Szegedy, 2015], which are problematic for the analysis of differential privacy guarantees in DP-SGD training because batch normalization causes each sample’s gradient to depend on all datapoints in the batch. As a substitute, we replaced BatchNorm layers with GroupNorm layers [Wu and He, 2018], and did so across all models for consistency. Finally, we modified the dimensions of the output layer of ResNet-18 to fit our patch size and binary classification requirements.

Experimental setup. The experiments were conducted using four V100 GPUs, each representing a client. In each scenario, training was conducted for 30 epochs with a mini-batch size of 32. All methods used the DP settings of $\sigma = 1.4$, $C = 0.7$, and $\delta = 10^{-5}$. Values for ϵ were then computed per-client based on the training set sizes in Table 1, and are provided in Table 2 (since several datapoints can be associated to the same patient, the formalism of group differential privacy [Dwork and Roth, 2014] could be applied to account for the correlations between such datapoints. For purposes of demonstration, and because the dataset we use is publicly available, we report ϵ as if each datapoint came from a distinct patient). FedAvg, AvgPush, CWT, Regular, Joint, and the proxy models of FML and ProxyFL used a DP-Adam optimizer with learning rate 0.001, whereas the private models of FML and ProxyFL used Adam with the same learning rate. The DML parameters α and β were set at 0.3 for both FML and ProxyFL. Finally, for FML and ProxyFL the private models are used to evaluate performance, the central model is used in the case of FedAvg, and for other methods the local models are used.

Results. The binary classification results for accuracy and macro-averaged accuracy are reported in Fig. 8 and Table 2. ProxyFL and FML achieve overall higher accuracy throughout training compared to other approaches, due to their private model’s ability to focus on local data while extracting useful information about other institutions through proxy models. Notably, FML’s performance peaks early and begins to degrade, while ProxyFL continues to improve marginally to the end of training.

5 Conclusion and Future Work

The recent surge in digitization of highly-regulated areas, such as healthcare and finance, is creating a large amount of data useful for training intelligent models. However, access to this data is limited due to regulatory and privacy concerns. In this paper, we proposed a novel decentralized federated learning scheme,

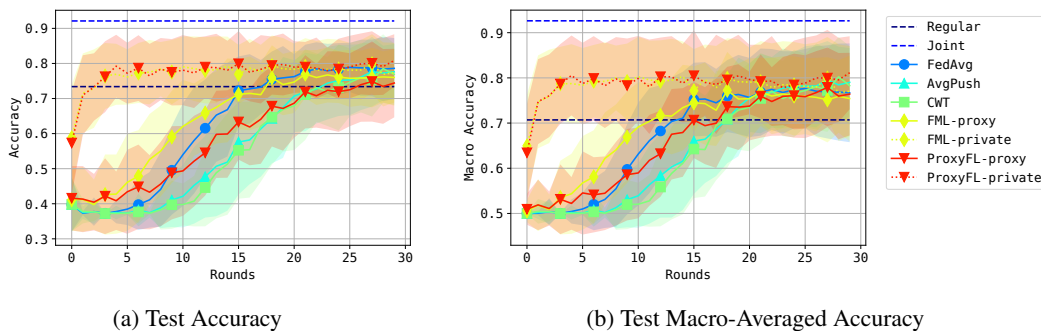


Figure 8: Performance of methods on the histopathology dataset involving four institutions. For (a) accuracy and (b) macro-averaged accuracy (b) the mean and standard deviation of performance on the test set is recorded at the end of each epoch. Each figure reports mean and standard deviation over 4 clients for each of 15 independent runs.

Method	Accuracy	Macro-accuracy	Client	Privacy Guarantees
Regular	0.734 ± 0.105	0.703 ± 0.132		$\sigma = 1.4, \delta = 10^{-5}$
AvgPush	0.776 ± 0.080	0.790 ± 0.076	C1	$\epsilon = 2.36$
CWT	0.769 ± 0.087	0.783 ± 0.087	C2	$\epsilon = 2.17$
FedAvg	0.786 ± 0.086	0.767 ± 0.109	C3	$\epsilon = 2.08$
FML	0.774 ± 0.085	0.770 ± 0.010	C4	$\epsilon = 2.12$
ProxyFL	0.808 ± 0.075	0.811 ± 0.081	Joint	$\epsilon = 1.00$
Joint	0.905 ± 0.030	0.913 ± 0.026		

Table 2: (Left) Final performance metrics on the histopathology dataset. (Right) Privacy guarantees for each client based on the training set sizes in Table 1. The guarantees are the same across all methods. This table reports mean and standard deviation over 4 clients for each of 15 independent runs.

ProxyFL, for multi-institutional collaborations without revealing participants’ private data. ProxyFL preserves data and model privacy, and provides a decentralized and communication-efficient mechanism for distributed training. Experiments suggest that ProxyFL is competitive compared to other baselines in terms of model accuracy, communication efficiency, and privacy preservation. Furthermore, we evaluated our approach on a real-world scenario consisting of four medical institutions collaborating to train models for identification of healthy vs. cancerous tissue from histopathology images.

In contrast to ProxyFL, some FL methods for private knowledge transfer require a public dataset [Papernot et al., 2017, Sun and Lyu, 2021]. This distinction is important, as the core issue in highly regulated domains is that large-scale public datasets are not readily available. Access to a public dataset greatly increases the variety of techniques that could be used, and is an avenue for future research. This work focused on the *privacy* aspects of the ProxyFL protocol, but not on its *security*. We have assumed that all clients collaborate in *good faith*. Handling malicious participants is another important direction of future research, and the ideas from Bhagoji et al. [2019] are relevant.

Finally, while differential privacy provides theoretical guarantees on the protection of privacy based on mathematical analysis, it is important to validate the effectiveness of these guarantees in practice. To be meaningful, such guarantees should demonstrably reduce the susceptibility of systems to reconstruction and membership inference attacks [Bhowmick et al., 2018]. Recent works use realistic privacy attacks to empirically test how much privacy is afforded by DP-SGD [Jagielski et al., 2020], while Nasr et al. [2021] demonstrate worst-case attacks that achieve the maximum privacy violation allowed by the theoretical guarantees of DP-SGD, but do not breach them. Testing and validation of privacy guarantees should be incorporated into model development and deployment processes.

Data Availability

All datasets used are publicly available. MNIST [LeCun et al., 1998], Fashion-MNIST [Xiao et al., 2017], and CIFAR-10 [Krizhevsky, 2009] are commonly used benchmarks for image classification with machine learning. The Kvasir dataset [Pogorelov et al., 2017] contains endoscopic images. Our histopathology study used some of the 1,399 WSIs from Camelyon-17 (Bánci et al. [2019]).

Code Availability

Python code of the proposed framework has been made available by Layer 6 AI (URL: <https://github.com/layer6ai-labs/ProxyFL>), and will be shared on the “Code and Data” section of Kimia Lab’s website (URL: <https://kimia.uwaterloo.ca/>).

Acknowledgments

SK and HT have been supported by The Natural Sciences and Engineering Research Council of Canada (NSERC). SK is also supported by a Vector Institute internship.

Author Contributions

S.K. conceptualized the idea of federated learning through proxy model sharing. J.W. enhanced communication efficiency through the PushSum scheme. J.C.C. contributed to the differential privacy analysis of the method. S.K., J.W., J.C.C. have equal contributions in the experimental analysis and paper writing. The contributions of J.W. were made while J.W. was at Layer 6. M.V. and H.R.T. were involved in the discussions of the approach, and provided critical feedback to the paper. H.R.T. discussed initial ideas with S.K., guided the histopathology experiments and external validations with histopathology images.

References

- Martin Abadi, Andy Chu, Ian Goodfellow, H Brendan McMahan, Ilya Mironov, Kunal Talwar, and Li Zhang. Deep learning with differential privacy. In *Proceedings of the 2016 ACM SIGSAC conference on computer and communications security*, pages 308–318, 2016.
- Mohammed Adnan, Shivam Kalra, Jesse C. Cresswell, Graham W. Taylor, and Hamid R. Tizhoosh. Federated learning and differential privacy for medical image analysis. *Scientific reports*, 12(1):1–10, 2022.
- Mathieu Andreux, Jean Ogier du Terrail, Constance Beguier, and Eric W Tramel. Siloed federated learning for multi-centric histopathology datasets. In *Domain Adaptation and Representation Transfer, and Distributed and Collaborative Learning*, pages 129–139. Springer, 2020.
- Mahmoud Assran, Nicolas Loizou, Nicolas Ballas, and Mike Rabbat. Stochastic gradient push for distributed deep learning. In *International Conference on Machine Learning*, pages 344–353. PMLR, 2019.
- Borja Balle, Gilles Barthe, Marco Gaboardi, Justin Hsu, and Tetsuya Sato. Hypothesis testing interpretations and Renyi differential privacy. In *Proceedings of the Twenty Third International Conference on Artificial Intelligence and Statistics*, volume 108, pages 2496–2506. PMLR, 2020.
- Arjun Nitin Bhagoji, Supriyo Chakraborty, Prateek Mittal, and Seraphin Calo. Analyzing federated learning through an adversarial lens. In *International Conference on Machine Learning*, pages 634–643. PMLR, 2019.
- Abhishek Bhowmick, John Duchi, Julien Freudiger, Gaurav Kapoor, and Ryan Rogers. Protection against reconstruction and its applications in private federated learning. *arXiv preprint arXiv:1812.00984*, 2018.

- Andrea Bizzego, Nicole Bussola, Marco Chierici, Valerio Maggio, Margherita Francescato, Luca Cima, Marco Cristoforetti, Giuseppe Jurman, and Cesare Furlanello. Evaluating reproducibility of ai algorithms in digital pathology with dapper. *PLoS computational biology*, 15(3):e1006269, 2019.
- David A. Bluemke, Linda Moy, Miriam A. Bredella, Birgit B. Ertl-Wagner, Kathryn J. Fowler, Vicky J. Goh, Elkan F. Halpern, Christopher P. Hess, Mark L. Schiebler, and Clifford R. Weiss. Assessing radiology research on artificial intelligence: a brief guide for authors, reviewers, and readers—From the Radiology editorial board. *Radiology*, 294(3):487–489, 2020. doi: 10.1148/radiol.2019192515.
- Péter Bándi, Oscar Geessink, Quirine Manson, Marcory Van Dijk, Maschenka Balkenhol, Meyke Hermesen, Babak Ehteshami Bejnordi, Byungjae Lee, Kyunghyun Paeng, Aoxiao Zhong, Quanzheng Li, Farhad Ghazvinian Zanjani, Svitlana Zinger, Keisuke Fukuta, Daisuke Komura, Vlado Ovtcharov, Shenghua Cheng, Shaoqun Zeng, Jeppe Thagaard, Anders B. Dahl, Huangjing Lin, Hao Chen, Ludwig Jacobsson, Martin Hedlund, Melih Çetin, Eren Halıcı, Hunter Jackson, Richard Chen, Fabian Both, Jörg Franke, Heidi Küsters-Vandeveld, Willem Vreuls, Peter Bult, Bram van Ginneken, Jeroen van der Laak, and Geert Litjens. From detection of individual metastases to classification of lymph node status at the patient level: The camelyon17 challenge. *IEEE Transactions on Medical Imaging*, 38(2):550–560, 2019. doi: 10.1109/TMI.2018.2867350.
- Nicholas Carlini and David Wagner. Towards evaluating the robustness of neural networks. In *2017 IEEE Symposium on Security and Privacy*, pages 39–57. IEEE, 2017.
- Nicholas Carlini, Chang Liu, Úlfar Erlingsson, Jernej Kos, and Dawn Song. The Secret Sharer: Evaluating and Testing Unintended Memorization in Neural Networks. In *Proceedings of the 28th USENIX Conference on Security Symposium, SEC’19*, page 267–284, USA, 2019. USENIX Association. ISBN 9781939133069.
- Ken Chang, Niranjana Balachandar, Carson Lam, Darvin Yi, James Brown, Andrew Beers, Bruce Rosen, Daniel L Rubin, and Jayashree Kalpathy-Cramer. Distributed deep learning networks among institutions for medical imaging. *Journal of the American Medical Informatics Association*, 25(8):945–954, 2018.
- Joseph Paul Cohen, Tianshi Cao, Joseph D Viviano, Chin-Wei Huang, Michael Fralick, Marzyeh Ghassemi, Muhammad Mamdani, Russell Greiner, and Yoshua Bengio. Problems in the deployment of machine-learned models in health care. *CMAJ*, 193(35):E1391–E1394, 2021.
- Jia Deng, Wei Dong, Richard Socher, Li-Jia Li, Kai Li, and Li Fei-Fei. Imagenet: A large-scale hierarchical image database. In *2009 IEEE Conference on Computer Vision and Pattern Recognition*, pages 248–255. IEEE, 2009.
- Cynthia Dwork and Aaron Roth. The algorithmic foundations of differential privacy. *Found. Trends Theor. Comput. Sci.*, 9(3–4):211–407, August 2014. ISSN 1551-305X. doi: 10.1561/04000000042.
- Cynthia Dwork, Krishnamurthy Kenthapadi, Frank McSherry, Ilya Mironov, and Moni Naor. Our data, ourselves: Privacy via distributed noise generation. In *Advances in Cryptology (EUROCRYPT 2006)*, volume 4004 of *Lecture Notes in Computer Science*, pages 486–503. Springer Verlag, May 2006a.
- Cynthia Dwork, Frank McSherry, Kobbi Nissim, and Adam Smith. Calibrating noise to sensitivity in private data analysis. In *Theory of Cryptography*, pages 265–284, Berlin, Heidelberg, 2006b. Springer Berlin Heidelberg. ISBN 978-3-540-32732-5.
- Cynthia Dwork, Guy N Rothblum, and Salil Vadhan. Boosting and differential privacy. In *2010 IEEE 51st Annual Symposium on Foundations of Computer Science*, pages 51–60. IEEE, 2010.
- Matt Fredrikson, Somesh Jha, and Thomas Ristenpart. Model inversion attacks that exploit confidence information and basic countermeasures. In *Proceedings of the 22nd ACM SIGSAC Conference on Computer and Communications Security, CCS ’15*, page 1322–1333, 2015. ISBN 9781450338325. doi: 10.1145/2810103.2813677.
- Richard L Graham, Timothy S Woodall, and Jeffrey M Squyres. Open MPI: A flexible high performance MPI. In *International Conference on Parallel Processing and Applied Mathematics*, pages 228–239. Springer, 2005.

- Otkrist Gupta and Ramesh Raskar. Distributed learning of deep neural network over multiple agents. *Journal of Network and Computer Applications*, 116:1–8, 2018.
- Kaiming He, Xiangyu Zhang, Shaoqing Ren, and Jian Sun. Deep residual learning for image recognition. In *Proceedings of the IEEE Conference on Computer Vision and Pattern Recognition (CVPR)*, June 2016.
- Geoffrey Hinton, Oriol Vinyals, and Jeff Dean. Distilling the knowledge in a neural network. *arXiv preprint arXiv:1503.02531*, 2015.
- Yutao Huang, Lingyang Chu, Zirui Zhou, Lanjun Wang, Jiangchuan Liu, Jian Pei, and Yong Zhang. Personalized cross-silo federated learning on non-IID data. In *Proceedings of the AAAI Conference on Artificial Intelligence*, volume 35-9, pages 7865–7873, 2021.
- Sergey Ioffe and Christian Szegedy. Batch normalization: Accelerating deep network training by reducing internal covariate shift. In *Proceedings of the 32nd International Conference on Machine Learning*, volume 37, pages 448–456, 2015.
- Matthew Jagielski, Jonathan Ullman, and Alina Oprea. Auditing differentially private machine learning: How private is private SGD? *Advances in Neural Information Processing Systems*, 33:22205–22216, 2020.
- Jing Ke, Yiqing Shen, and Yizhou Lu. Style normalization in histology with federated learning. In *2021 IEEE 18th International Symposium on Biomedical Imaging (ISBI)*, pages 953–956. IEEE, 2021.
- Christopher J Kelly, Alan Karthikesalingam, Mustafa Suleyman, Greg Corrado, and Dominic King. Key challenges for delivering clinical impact with artificial intelligence. *BMC medicine*, 17(1):1–9, 2019.
- David Kempe, Alin Dobra, and Johannes Gehrke. Gossip-based computation of aggregate information. In *44th Annual IEEE Symposium on Foundations of Computer Science, 2003. Proceedings.*, pages 482–491. IEEE, 2003.
- Diederik P Kingma and Jimmy Ba. Adam: A method for stochastic optimization. In *International Conference on Learning Representations*, 2014.
- Alex Krizhevsky. Learning Multiple Layers of Features from Tiny Images. *Technical Report, University of Toronto, Toronto*, 2009.
- Yann LeCun, Léon Bottou, Yoshua Bengio, and Patrick Haffner. Gradient-based learning applied to document recognition. *Proceedings of the IEEE*, 86(11):2278–2324, 1998.
- Chengxi Li, Gang Li, and Pramod K. Varshney. Decentralized federated learning via mutual knowledge transfer. *IEEE Internet of Things Journal*, 9(2):1136–1147, 2022. doi: 10.1109/JIOT.2021.3078543.
- Tian Li, Anit Kumar Sahu, Ameet Talwalkar, and Virginia Smith. Federated learning: Challenges, methods, and future directions. *IEEE Signal Processing Magazine*, 37(3):50–60, 2020a.
- Wenqi Li, Fausto Milletari, Daguang Xu, Nicola Rieke, Jonny Hancox, Wentao Zhu, Maximilian Baust, Yan Cheng, Sébastien Ourselin, M Jorge Cardoso, et al. Privacy-preserving federated brain tumour segmentation. In *International Workshop on Machine Learning in Medical Imaging*, pages 133–141, 2019.
- Xiaoxiao Li, Yufeng Gu, Nicha Dvornek, Lawrence H. Staib, Pamela Ventola, and James S. Duncan. Multi-site fMRI analysis using privacy-preserving federated learning and domain adaptation: ABIDE results. *Medical Image Analysis*, 65:101765, 2020b. ISSN 1361-8415. doi: <https://doi.org/10.1016/j.media.2020.101765>.
- Tao Lin, Lingjing Kong, Sebastian U Stich, and Martin Jaggi. Ensemble distillation for robust model fusion in federated learning. In *Advances in Neural Information Processing Systems*, volume 33, pages 2351–2363, 2020.

- Ming Y. Lu, Richard J. Chen, Dehan Kong, Jana Lipkova, Rajendra Singh, Drew F.K. Williamson, Tiffany Y. Chen, and Faisal Mahmood. Federated learning for computational pathology on gigapixel whole slide images. *Medical Image Analysis*, 76:102298, 2022. ISSN 1361-8415. doi: <https://doi.org/10.1016/j.media.2021.102298>.
- Jiaxin Ma, Ryo Yonetani, and Zahid Iqbal. Adaptive distillation for decentralized learning from heterogeneous clients. In *2020 25th International Conference on Pattern Recognition (ICPR)*, pages 7486–7492. IEEE, 2021.
- Liam G McCoy, John D Banja, Marzyeh Ghassemi, and Leo Anthony Celi. Ensuring machine learning for healthcare works for all. *BMJ Health & Care Informatics*, 27(3), 2020.
- H. Brendan McMahan, Eider Moore, Daniel Ramage, Seth Hampson, and Blaise Aguera y Arcas. Communication-Efficient Learning of Deep Networks from Decentralized Data. In *Proceedings of the 20th International Conference on Artificial Intelligence and Statistics (AISTATS)*, 2017.
- H. Brendan McMahan, Daniel Ramage, Kunal Talwar, and Li Zhang. Learning differentially private recurrent language models. In *International Conference on Learning Representations*, 2018.
- Luca Melis, Congzheng Song, Emiliano De Cristofaro, and Vitaly Shmatikov. Exploiting unintended feature leakage in collaborative learning. In *2019 IEEE Symposium on Security and Privacy (SP)*, pages 691–706. IEEE, 2019.
- Ilya Mironov. Rényi differential privacy. *2017 IEEE 30th Computer Security Foundations Symposium (CSF)*, Aug 2017. doi: 10.1109/csf.2017.11.
- Ilya Mironov, Kunal Talwar, and Li Zhang. Rényi Differential Privacy of the Sampled Gaussian Mechanism. *arXiv preprint arXiv:1908.10530*, 2019.
- Milad Nasr, Shuang Songi, Abhradeep Thakurta, Nicolas Papernot, and Nicholas Carlini. Adversary instantiation: Lower bounds for differentially private machine learning. In *2021 IEEE Symposium on Security and Privacy (SP)*, pages 866–882, 2021. doi: 10.1109/SP40001.2021.00069.
- Angelia Nedić and Alex Olshevsky. Stochastic gradient-push for strongly convex functions on time-varying directed graphs. *IEEE Transactions on Automatic Control*, 61(12):3936–3947, 2016.
- Angelia Nedić, Alex Olshevsky, and Michael G. Rabbat. Network topology and communication-computation tradeoffs in decentralized optimization. *Proceedings of the IEEE*, 106(5):953–976, 2018. doi: 10.1109/JPROC.2018.2817461.
- Nicolas Papernot, Martín Abadi, Úlfar Erlingsson, Ian Goodfellow, and Kunal Talwar. Semi-supervised knowledge transfer for deep learning from private training data. In *Proceedings of the International Conference on Learning Representations*, 2017.
- Seong Ho Park and Kyunghwa Han. Methodologic guide for evaluating clinical performance and effect of artificial intelligence technology for medical diagnosis and prediction. *Radiology*, 286(3):800–809, 2018.
- Konstantin Pogorelov, Kristin Ranheim Randel, Carsten Griwodz, Sigrun Losada Eskeland, Thomas de Lange, Dag Johansen, Concetto Spampinato, Duc-Tien Dang-Nguyen, Mathias Lux, Peter Thelin Schmidt, et al. Kvasir: A multi-class image dataset for computer aided gastrointestinal disease detection. In *Proceedings of the 8th ACM on Multimedia Systems Conference*, pages 164–169, 2017.
- Pranav Rajpurkar, Jian Zhang, Konstantin Lopyrev, and Percy Liang. SQuAD: 100,000+ Questions for Machine Comprehension of Text. In *EMNLP*, pages 2383–2392, 2016.
- E. Seneta. *Non-negative Matrices and Markov Chains*. Springer Series in Statistics. Springer New York, 2006. ISBN 9780387327921.
- Tao Shen, Jie Zhang, Xinkang Jia, Fengda Zhang, Gang Huang, Pan Zhou, Kun Kuang, Fei Wu, and Chao Wu. Federated mutual learning. *arXiv preprint arXiv:2006.16765*, 2020.

- Lichao Sun and Lingjuan Lyu. Federated model distillation with noise-free differential privacy. In *Proceedings of the Thirtieth International Joint Conference on Artificial Intelligence, IJCAI-21*, pages 1563–1570, 2021.
- Hamid Reza Tizhoosh and Liron Pantanowitz. Artificial intelligence and digital pathology: Challenges and opportunities. *Journal of Pathology Informatics*, 9, 2018.
- TorchVision. Torchvision: Pytorch’s computer vision library. <https://github.com/pytorch/vision>, 2016.
- Stacey Truex, Ling Liu, Mehmet Emre Gursoy, Lei Yu, and Wenqi Wei. Demystifying membership inference attacks in machine learning as a service. *IEEE Transactions on Services Computing*, pages 1–1, 2019. doi: 10.1109/TSC.2019.2897554.
- Kerstin N Vokinger, Stefan Feuerriegel, and Aaron S Kesselheim. Mitigating bias in machine learning for medicine. *Communications Medicine*, 1(1):1–3, 2021.
- Stefanie Warnat-Herresthal, Hartmut Schultze, Krishnaprasad Lingadahalli Shastri, Sathyanarayanan Manamohan, Saikat Mukherjee, Vishesh Garg, Ravi Sarveswara, Kristian Händler, Peter Pickkers, N Ahmad Aziz, et al. Swarm learning for decentralized and confidential clinical machine learning. *Nature*, 594(7862):265–270, 2021.
- Thorsten Wittkopp and Alexander Acker. Decentralized federated learning preserves model and data privacy. In *International Conference on Service-Oriented Computing*, pages 176–187. Springer, 2020.
- Yuxin Wu and Kaiming He. Group normalization. In *Proceedings of the European Conference on Computer Vision (ECCV)*, September 2018.
- Han Xiao, Kashif Rasul, and Roland Vollgraf. Fashion-MNIST: a novel image dataset for benchmarking machine learning algorithms. *arXiv preprint arXiv:1708.07747*, 2017.
- Qian Yang, Jianyi Zhang, Weituo Hao, Gregory P Spell, and Lawrence Carin. Flop: Federated learning on medical datasets using partial networks. In *Proceedings of the 27th ACM SIGKDD Conference on Knowledge Discovery & Data Mining*, pages 3845–3853, 2021.
- Lei Yu, Ling Liu, Calton Pu, Mehmet Emre Gursoy, and Stacey Truex. Differentially private model publishing for deep learning. In *2019 IEEE Symposium on Security and Privacy (SP)*, pages 332–349. IEEE, 2019.
- Mikhail Yurochkin, Mayank Agarwal, Soumya Ghosh, Kristjan Greenewald, Nghia Hoang, and Yasaman Khazaeni. Bayesian nonparametric federated learning of neural networks. In *International Conference on Machine Learning*, pages 7252–7261. PMLR, 2019.
- Ying Zhang, Tao Xiang, Timothy M Hospedales, and Huchuan Lu. Deep mutual learning. In *Proceedings of the IEEE Conference on Computer Vision and Pattern Recognition*, pages 4320–4328, 2018.

Appendix

A Experiment Details

A.1 Benchmark Image Classification

We used the model architectures from Shen et al. [2020] for direct comparison. Specifically, the MLP consists of two hidden layers with 200 units each and ReLU activations. The CNN1 model consists of (conv(3×3, 6), ReLU, maxpool(2×2), conv(3×3, 16), ReLU, maxpool(2×2), fc(64), ReLU, fc(10)) where conv(3×3, 6) means a 3×3 convolution layer with 6 channels, maxpool(2×2) is a max pooling layer with 2×2 kernel, and fc(64) means a fully connected layer with 64 hidden units, etc. The CNN2 model is (conv(3×3, 128), ReLU, maxpool(2×2), conv(3×3, 128), ReLU, maxpool(2×2), fc(10)).

B Additional Results

B.1 Benchmark Image Classification

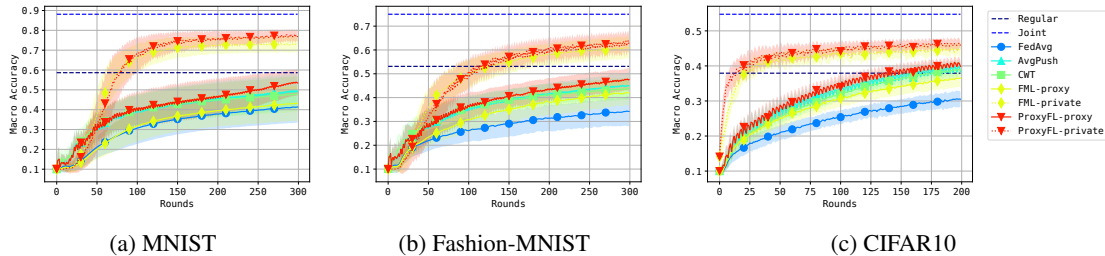


Figure 9: Macro-accuracy of the test performance with DP training. Each figure reports mean and standard deviation over 8 clients for each of 5 independent runs.

In this section we provide additional experimental results for benchmarking on common image classification datasets. Fig. 9 shows the macro-accuracies, similar to the accuracies shown in the main text. Macro-accuracy is computed by first evaluating the accuracy per class then averaging the class accuracies. In settings with imbalanced data, it can be easy to achieve high accuracies without meaningful learning, whereas high macro-accuracy requires good performance on all classes. In our experiments classes are imbalanced with each client having a majority class. Nevertheless, we see that the macro-accuracies are very similar to the accuracies in the main text, showing that the methods are not biased towards the majority class.

Next we show additional ablation studies on MNIST. In the main text the private models for ProxyFL and FML were different from the proxy/centralized models. Fig. 10 shows the training curves when all models used the same MLP architecture. We see that ProxyFL-private can achieve the best performance regardless of the private model structure, as compared with the main text.

Increasing mini-batch size is beneficial for the stability of stochastic gradient updates and for computation speed. However, smaller batch sizes lead to stronger (ϵ, δ) privacy guarantees when using DP-SGD [Abadi et al., 2016]. In the main text, for computation efficiency we used $B = 250$ images per DP-SGD step. Fig. 11 shows how batch size can affect the privacy guarantee. Smaller batch sizes do not have a significant effect on the final accuracy of ProxyFL-private, while the privacy guarantee dramatically improves. Therefore, we can have a strong privacy guarantee with ProxyFL by using small batch sizes at the cost of longer training time.

Finally, Fig. 12 shows the performance with different DML weights α, β . Note that this only affects ProxyFL and FML. We fix $\alpha = \beta$ in the experiments. We can see that ProxyFL outperforms its centralized counterpart FML for all values of α . With a larger α , the performance gap between the private and proxy models gets smaller, which is reasonable as they tend to mimic each other.

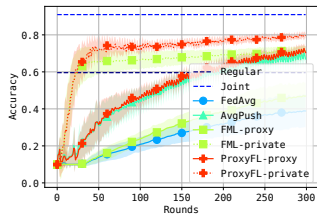


Figure 10: Accuracy when both private and proxy models are MLPs. This figure reports mean and standard deviation over 8 clients for each of 5 independent runs.

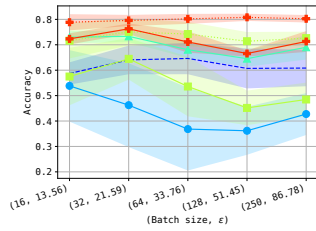


Figure 11: Effect of batch size. This figure reports mean and standard deviation over 8 clients for each of 5 independent runs.

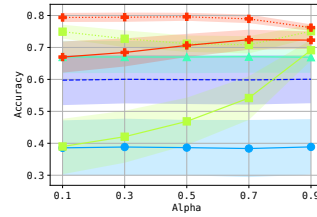


Figure 12: Effect of DML weight. This figure reports mean and standard deviation over 8 clients for each of 5 independent runs.

B.2 Histopathology Image Analysis

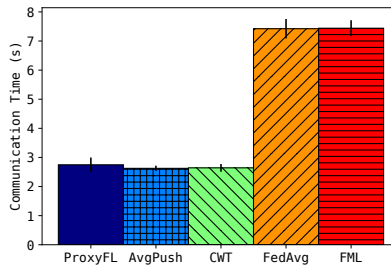


Figure 13: The total communication time per client. Federated Averaging (FedAvg) and Federated Mutual Learning (FML) have less efficient communication because all clients need to communicate with a single server, causing a bottleneck, whereas the other methods are decentralized. This figure reports mean and standard deviation over 4 clients for each of 15 independent runs.

We measured the communication time required by each method in Fig. 13. ProxyFL is more communication efficient than FedAvg and FML, because it avoids a bottleneck at the central server. In centralized methods the central server must sequentially communicate with all clients to receive their models, and again to send the updated version back. In ProxyFL and the other decentralized approaches, each client only needs to send and receive a single model per round.